Report

Current Biology

Humidity Sensing in *Drosophila*

Graphical Abstract

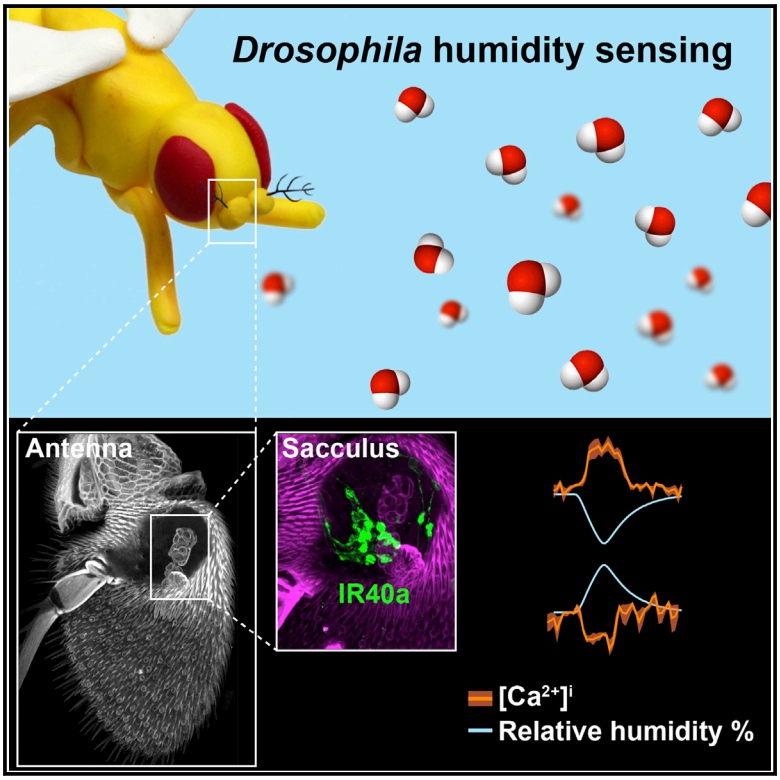

Highlights

- *Drosophila* species prefer distinct humidity ranges, related to their native habitat
- The ionotropic receptors IR25a, IR93a, and IR40a are all required for RH preference
- RH changes are sensed by IR40a neurons in the sacculus, an antennal substructure
- RH and temperature are processed by different cells in the *Drosophila* antenna

Authors

Anders Enjin, Emanuela E. Zaharieva, Dominic D. Frank, Suzan Mansourian, Greg S.B. Suh, Marco Gallio, Marcus C. Stensmyr

Correspondence

marco.gallio@northwestern.edu (M.G.), marcus.stensmyr@biol.lu.se (M.C.S.)

In Brief

Enjin et al. describe genes and neurons necessary for humidity responses in *Drosophila*. Humidity responses require the ionotropic receptors IR25a, IR93a, and IR40a, expressed in specialized neurons of the antennal sacculus. Humidity preference is innate and species specific: "desert" flies prefer a drier environment, while "rainforest" flies prefer a humid one.

Enjin et al., 2016, Current Biology *26*, 1352–1358
May 23, 2016
http://dx.doi.org/10.1016/j.cub.2016.03.049

CellPress

Current Biology
Report

Humidity Sensing in *Drosophila*

Anders Enjin,[1] Emanuela E. Zaharieva,[2] Dominic D. Frank,[2] Suzan Mansourian,[1] Greg S.B. Suh,[3] Marco Gallio,[2,*] and Marcus C. Stensmyr[1,*]

[1]Department of Biology, Lund University, 22362 Lund, Sweden
[2]Department of Neurobiology, Northwestern University, Evanston, IL 60208, USA
[3]Skirball Institute of Biomolecular Medicine, Neuroscience Institute, Department of Cell Biology, New York University School of Medicine, New York, NY 10016, USA
*Correspondence: marco.gallio@northwestern.edu (M.G.), marcus.stensmyr@biol.lu.se (M.C.S.)
http://dx.doi.org/10.1016/j.cub.2016.03.049

SUMMARY

Environmental humidity influences the fitness and geographic distribution of all animals [1]. Insects in particular use humidity cues to navigate the environment, and previous work suggests the existence of specific sensory mechanisms to detect favorable humidity ranges [2–5]. Yet, the molecular and cellular basis of humidity sensing (hygrosensation) remains poorly understood. Here we describe genes and neurons necessary for hygrosensation in the vinegar fly *Drosophila melanogaster*. We find that members of the *Drosophila* genus display species-specific humidity preferences related to conditions in their native habitats. Using a simple behavioral assay, we find that the ionotropic receptors IR40a, IR93a, and IR25a are all required for humidity preference in *D. melanogaster*. Yet, whereas IR40a is selectively required for hygrosensory responses, IR93a and IR25a mediate both humidity and temperature preference. Consistent with this, the expression of IR93a and IR25a includes thermosensory neurons of the arista. In contrast, IR40a is excluded from the arista but is expressed (and required) in specialized neurons innervating pore-less sensilla of the sacculus, a unique invagination of the third antennal segment. Indeed, calcium imaging showed that IR40a neurons directly respond to changes in humidity, and IR40a knockdown or IR93a mutation reduced their responses to stimuli. Taken together, our results suggest that the preference for a specific humidity range depends on specialized sacculus neurons, and that the processing of environmental humidity can happen largely in parallel to that of temperature.

RESULTS

Humidity Preference Is Innate and Species Specific

To test the humidity preference of *Drosophila*, we devised a behavioral assay where flies are given a choice between different levels of relative humidity (RH). We took advantage of the hygroscopic features of super-saturated salt solutions [6] and created niches with different RH levels in a multi-well plate (Figure 1A; see legend for details). Super-saturated solutions of LiCl, NaCl, or KH_2PO_4 yielded stable levels of ~20%, ~70%, and ~85% RH, respectively, while headspace above the wells remained at constant temperature (Figures 1B and 1C) and did not contain detectable volatiles (not shown), providing a simple test for humidity preference. When confronted with the choice between 20% and 70% RH, wild-type *D. melanogaster* consistently chose the moist side, so that after 4 hr almost all flies were at 70% RH (Figure 1D). In contrast, when given a choice between 70% and 85%, flies preferred the drier side (Figure 1E). This is broadly consistent with previous reports [7], and suggests that flies have an innate preference for ~70% RH over 20% and 85%.

If this represents an innate preference, different species of *Drosophila* should display predictable humidity preference in accordance with the climate of their native habitat. Thus, we next tested the afrotropical species *Drosophila teissieri*—native to humid rainforests in west equatorial Africa—and *Drosophila mojavensis*—native to the dry Sonoran desert of the Southwestern United States and Mexico (Figure 1F). Strikingly, *D. mojavensis* preferred 20% over 70% RH, whereas *D. teissieri* showed a preference for 85% RH over 70% RH (Figures 1G and 1H). Taken together, these results suggest that drosophilids have innate and species-specific humidity preferences.

IR25a, *IR93a*, and *IR40a* Are Necessary for Humidity Preference

The transient receptor potential channels water witch (*wtrw*) and nanchung (*nan*) have previously been implicated in the response to extreme humidity conditions (0% versus 100% RH) [8]. Yet, when given a choice between 20% and 70% RH, $wtrw^1$ and nan^{36a} mutants showed a preference for the humid side (Figure 1I). Compared to controls, this preference was quantitatively reduced; nevertheless, the mutants retained the ability to detect humidity differences. We conclude that these genes are unlikely the main mediators of hygrosensory responses in *Drosophila* (see also [9]).

Previous work has pointed to the fly antenna as a key organ for the detection of humidity in insects [4, 5]. Most sensory neurons of the antenna express receptor proteins of the odorant receptor (OR) [10, 11] or ionotropic receptor (IR) families [12], and broadly expressed co-receptors are typically required for function: Orco for ORs [13] and IR8a or IR25a for IRs [14]. Thus, we reasoned that testing mutants for these co-receptors in our assay could narrow down the number of candidate humidity receptors. Both $Orco^2$ and $IR8a^1$ mutants showed normal preference. In

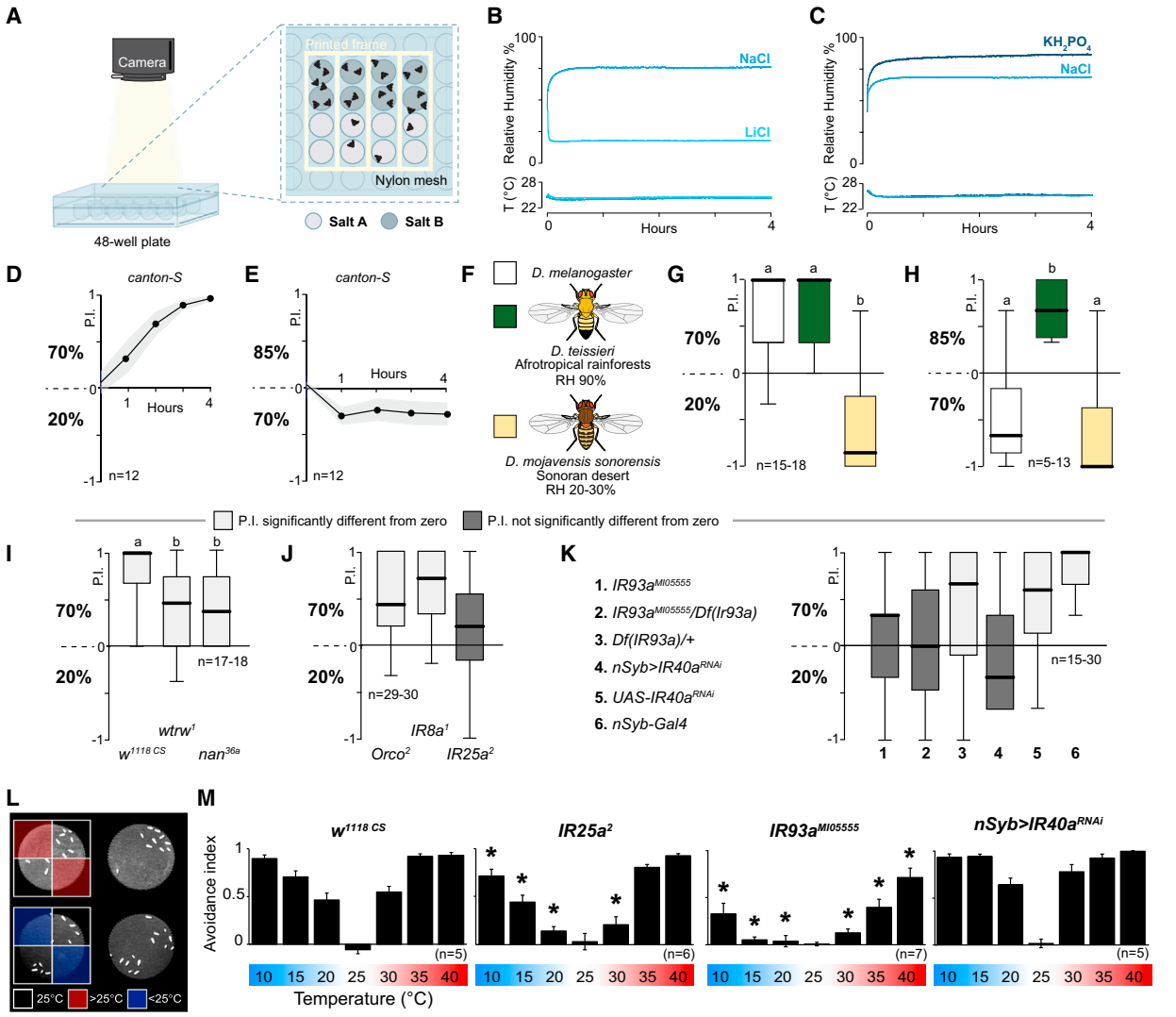

Figure 1. Innate Humidity Preference in Drosophilids

(A) Schematic drawing of our humidity-preference assay. The arena uses the hygroscopic features of super-saturated salt solutions to create niches with different humidity levels. Forty-eight-well plates, filled with salt solutions, are covered by a fine nylon mesh for the flies to walk on without being able to reach the liquid in the wells. Flies are placed in the arena and provided with the choice between two different RH ranges, while a camera images their position for 4 hr.

(B) Example humidity and temperature traces measured from the arena with saturated solutions of LiCl and NaCl.

(C) Example humidity and temperature traces measured from the arena with saturated solutions of NaCl and KH_2PO_4.

(D and E) Humidity-preference index of male Canton-S flies tested in the arena with RH 20% versus RH 70% (D) and RH 70% versus RH 85% (E). Shaded areas represent SEM.

(F) Drawings of *D. teissieri* and *D. mojavensis*.

(G and H) Humidity-preference index after 4 hr of *D. melanogaster*, *D. teissieri*, and *D. mojavensis* tested in a humidity-preference arena with RH 20% and RH 70% (G) and RH 70% and RH 85% (H).

(I) Humidity-preference index of $w^{1118\ CS}$, $wtrw^{1}$, and nan^{36a} tested in a humidity-preference arena with RH 20% and RH 70%.

(J) Humidity-preference index of $Orco^{2}$, $IR8a^{1}$, and $IR25a^{2}$.

(K) Humidity-preference index of $IR93a^{MI05555}$ and $nSyb{>}IR40a^{RNAi}$ and genetic background controls. See also Figure S1A.

(L) Overview of the temperature-preference assay.

(M) Temperature-avoidance index of $w^{1118\ CS}$, $IR25a^{2}$, $IR93a^{MI05555}$, and $nSyb{>}IR40a^{RNAi}$. See also Figure S1B.

Humidity preference was tested with one-sample t test, theoretical mean 0; $p < 0.05$ was considered significant. Differences between $w^{1118\ CS}$ and $wtrw^{1}$ or nan^{36a} were tested with one-way ANOVA with Bonferroni correction; b denotes $p < 0.01$. The edges of the boxes are the first and third quartiles, thick lines mark the medians, and whiskers represent data range. Temperature-avoidance index values were compared by ANOVA; asterisks denote a significant difference between the mutant and genetic background control ($w^{1118\ CS}$), $p < 0.01$. $nSyb{>}IR40a^{RNAi}$ scores were compared by two-way ANOVA with relevant *nSyb-Gal4*/+ and $UAS\text{-}IR40a^{RNAi/+}$ controls (Figure S1B), demonstrating no significant interaction; error bars indicate mean ± SEM. P.I., preference index.

contrast, humidity preference was essentially abolished in *IR25a*^{2} mutants (Figure 1J).

IR25a is associated with seven specific receptors. Four of these (IR41a, IR75d, IR76a, and IR92a) have well-described high-affinity volatile ligands [15]. Three IR25a-dependent receptors, IR21a, IR93a, and IR40a, instead remain orphan. Thus, we next tested whether mutations in these genes affect humidity preference. An *IR21a* mutant (*IR21a*^{EP526}) showed normal humidity preference (Figure S1A). In contrast, *IR93a* mutants (*IR93a*^{MI05555} and *IR93a*^{MI05555}*/Df(IR93a)*) displayed strong humidity-preference defects (Figure 1K). *IR40a* mutants are not available, yet RNAi-mediated knockdown of IR40a throughout the nervous system (i.e., in *n-synaptobrevin-Gal4>UAS-IR40a*^{RNAi} flies) also strongly affected humidity preference (Figure 1K). Thus, we conclude that IR25a, IR93a, and IR40a are all required for humidity-preference behavior.

Hygrosensation has previously been proposed to comprise a thermosensory component [5, 16]. Hence, we next set out to determine whether IR21a, IR25a, IR93a, and IR40a also mediate temperature responses. We used a two-choice test for temperature preference, assaying a wide range of test temperatures (10°C–40°C, in 5°C steps) over the preferred 25°C (Figure 1L) [17, 18]. In this assay, *IR21a*^{EP526}, *IR25a*^{2}, and *IR93a*^{MI05555} mutant flies displayed significant temperature-preference defects in both hot and cold ranges (Figure 1M; Figure S1B). In contrast, despite a strong humidity-preference phenotype, *nSyb>IR40a*^{RNAi} flies reported a normal temperature preference (Figure 1M; Figure S1B). We conclude that IR25a and IR93a are required for both humidity and temperature preference, whereas IR40a is selectively required for hygrosensory responses.

Humidity Responses Are Mediated by No-Pore Sensilla of the Sacculus

Our next goal was to discover the cellular substrates for hygrosensation. Based on the mutant phenotypes described above, we hypothesized that the sensory neurons mediating humidity responses co-express IR25a, IR93a, and IR40a. Consistent with a role as co-receptor, IR25a expression is broad, and includes olfactory neurons in the third antennal segment, thermosensory neurons of the arista, and neurons innervating the sacculus [12]. Previous work has shown that IR40a and IR93a are indeed co-expressed in a small group of cells surrounding the sacculus (a unique invagination of the third antennal segment), and this structure has been suggested to contain hygroreceptors [19]. Hence, we set out to determine the organization of the IR-expressing sacculus neurons. Gal4 drivers are available that recapitulate the expression of IR25a and IR40a, whereas previous attempts to produce *IR93a-Gal4* have been unsuccessful [14, 15]. Here we used two different IR93a drivers representing extremes of the range of expression we observed in search of a faithful driver for IR93a-expressing cells. *IR93a-LexA* labels neurons targeting the sacculus and all thermoreceptors of the arista, whereas *VT044927-Gal4* (derived from a single IR93a enhancer) is expressed in a handful of sacculus neurons and in a variable number of cells in the arista (see Figure S2 for further validation of the expression of these genes in the antenna). The sacculus is composed of three chambers (Figures 2A and 2C), each housing sensilla with distinct morphology. Those housed in chambers I and II are of the so-called no-pore type (Figures 2B and 2D), are innervated by two or three neurons, and show similarity to hygrosensilla of other insects [19]. To examine which sensilla and chambers are innervated by neurons expressing IR25a, IR93a, and IR40a, we expressed CD8:GFP under the control of each driver and analyzed intact antennae by confocal microscopy. *IR25a-Gal4* labeled most neurons innervating chambers I–III of the sacculus, as well as all thermosensors of the arista (Figures 2E and 2G; [18]). In contrast, *IR40a-Gal4* exclusively labeled cells targeting the no-pore sensilla located in chambers I and II (Figure 2F). Specifically, *IR40a-Gal4* labeled one cell per sensillum in chamber I, and two cells per sensillum in chamber II (Figure 2G). The *IR93a-LexA* driver labeled two or three cells per sensillum in both chambers I and II (data not shown), whereas the more selective *VT044927-Gal4* driver was active in a subset of chamber I neurons and only one cell/sensillum in chamber II (Figure 2G). Cell counts in animals expressing GFP under the control of both *IR40a-* and *VT044927-Gal4* revealed similar numbers, suggesting that *VT044927-Gal4* is expressed in a subpopulation of *IR40a-Gal4* cells (Figure 2G). We conclude that IR25a, IR93a, and IR40a are likely co-expressed in neurons targeting chambers I and II.

These IR drivers also gave us the opportunity to directly test in which cell type the activity of IR40a may be required to mediate humidity preference, i.e., by targeted knockdown using *IR40a*^{RNAi}. Driving *IR40a*^{RNAi} in *IR25a-* or *IR40a-Gal4* cells produced flies in which humidity preference was abolished (Figure 2H), and a similar effect was observed when *UAS-IR40a*^{RNAi} was expressed under the control of the narrowly expressed *VT044927* driver. Moreover, expression of a *UAS-IR93a* transgene under the control of this driver was sufficient to rescue the humidity-preference phenotype of *IR93a*^{MI05555}*/Df(IR93a)* mutants (Figure 2H), indicating that IR40a and IR93a are required in a relatively small number of chamber I/II sacculus neurons to mediate humidity preference.

Sacculus Neurons Project to Distinct Glomeruli in the Posterior Antennal Lobe

In which region of the fly brain are humidity stimuli represented? To address this question, we used *IR25a-* and *IR40a-Gal4* to express CD8:GFP, and followed labeled axons from the antenna to the brain. *IR25a>GFP* projections innervated a subset of olfactory glomeruli of the antennal lobe (not shown), as well as the "hot" and "cold" glomeruli of the posterior antennal lobe (PAL) (Figure 3A) [18]. In addition, *IR25a-Gal4* also labeled two glomeruli of unusual shape, previously described as "Arm" (or VP4) and "Column" (or VP1) (Figures 3A and 3B) [15, 20]. *IR40a>GFP* termini were prominent in both the Arm and Column, but did not target the hot or cold glomeruli of the PAL (Figures 3C–3E). Both *IR93a-LexA* and *VT044927-Gal4* also labeled projections innervating the Arm and Column, as well as thermosensory glomeruli (data not shown). Hence, given the selective requirement for IR40a in humidity preference, the Arm and Column are candidate glomeruli for the representation of humidity.

The Arm Glomerulus Responds to Dry Air

To determine which structures in the brain are activated by humidity changes, we first used the fluorescent calcium sensor CaMPARI [21]. When bound to calcium, the CaMPARI protein can be converted from green to red by 400-nm light illumination,

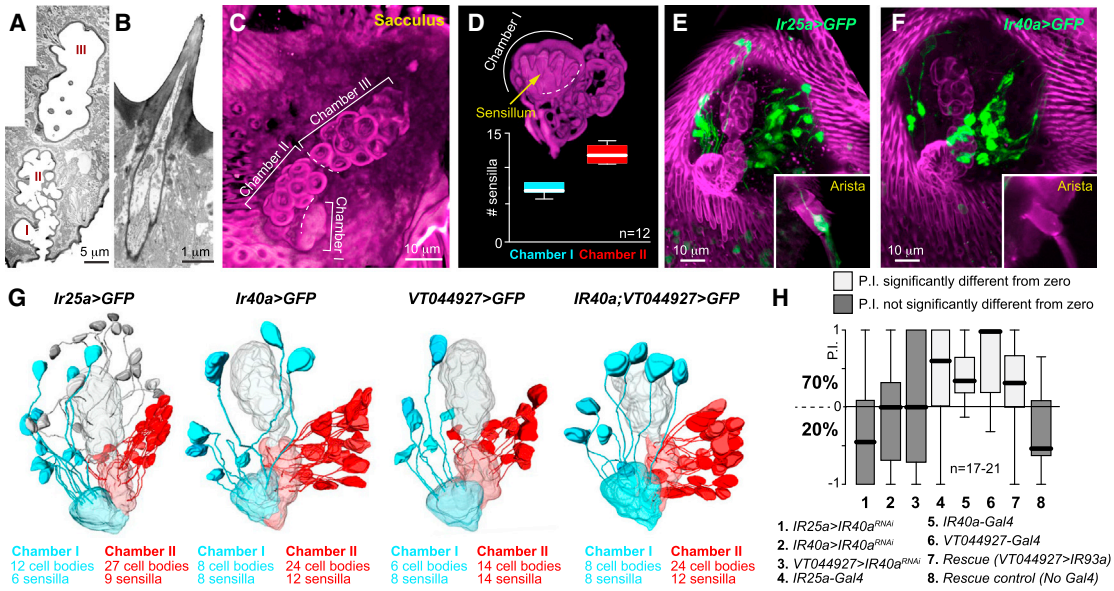

Figure 2. IR93a and IR40a Are Required in Sacculus Chambers I and II for Humidity-Preference Behavior

(A) Transmission electron microscope (TEM) micrograph of a section of the third antennal segment transecting the sacculus. This structure is composed of three chambers (I–III), each housing sensilla with distinct morphology.

(B) TEM micrograph showing a no-pore sensillum basiconicum in chamber I of the sacculus. Each sensillum is innervated by two or three neurons, whose outer dendritic segments completely fill the lumen.

(C) Maximum-intensity projection of cuticular autofluorescence showing the outline of the sacculus.

(D) Three-dimensional model of the sacculus based on (C), and quantification of sensilla in chambers I and II. The edges of the boxes are the first and third quartiles, thick lines mark the medians, and whiskers represent data range.

(E and F) Maximum-intensity projection of antennae from *IR25a>GFP* (E) and *IR40a>GFP* (F). Insets show arista. See also Figure S2.

(G) Three-dimensional reconstruction of cells innervating the sacculus in *IR25a>GFP*, *IR40a>GFP*, *VT044927>GFP*, and *VT044927-Gal4/IR40a-Gal4>GFP*.

(H) Humidity-preference index of *IR25a>IR40a^{RNAi}*, *IR40a>IR40a^{RNAi}*, *VT044927>IR40a^{RNAi}*, rescue of *IR93a* (*UAS-IR93a;IR93a^{MI05555}/Df(IR93a)*, *VT044927-Gal4*), and genetic background controls. The edges of the boxes are the first and third quartiles, thick lines mark the medians, and whiskers represent data range. Preference was tested with one-sample t test, theoretical mean 0, $p < 0.05$, light boxplots; dark boxplots indicate no significant preference.

persistently labeling neurons that are active (i.e., neurons with high intracellular calcium) during the temporal window of illumination. We expressed CaMPARI under the control of *IR25a-Gal4*, and exposed flies to fast changes in humidity at constant temperature (Figure S3A) while simultaneously illuminating the fly head. When *IR25a>CaMPARI$^{(V398D)}$* flies were exposed to a dry stimulus, we observed consistent photoconversion of the Arm glomerulus but no conversion of the Column (Figures 3F–3H). Humid stimuli, on the other hand, failed to consistently photoconvert any structures labeled by our *IR25a-Gal4* line (data not shown).

Next, we used two-photon calcium imaging to determine the dynamic response of the Arm glomerulus to changes in humidity, by expressing the calcium indicator GCaMP6m under the control of *IR40a-Gal4* (Figures 3I and 3J). In accordance with the CaMPARI results, the Arm responded with a rapid, reversible calcium increase to dry-air stimuli (Figure 3K). Interestingly, the same glomerulus also responded to humid air, but this time with a corresponding decrease in $[Ca^{2+}]^i$ (Figure 3K). As in CaMPARI, the Column did not show specific responses to changes in humidity (Figure 3L). Calcium imaging experiments from flies expressing GCaMP6m under the control of the *IR25a-Gal4* and *VT044927-Gal4* drivers produced similar results (i.e., we observed responses to dry air limited to the Arm and no Ca^{2+} increases in response to humid air stimuli; Figures S3B–S3D and data not shown). Next, we asked whether IR40a and IR93a are required for the dynamic responses of the Arm glomerulus to dry air. Indeed, responses recorded in the Arm glomerulus were reduced (albeit not abolished) in *IR93a^{MI05555}* and *IR40a^{RNAi}* flies (Figure 3M). The fact that calcium responses were not entirely abolished (vis-à-vis the behavioral phenotypes of both *IR93a^{MI05555}* and *IR40a^{RNAi}* knockdown) may indicate that behavior requires a rather finely tuned hygrosensory input, or perhaps reflects the different timescales of functional imaging and behavioral testing.

In a previous study, IR40a was suggested as the receptor for the insect repellent *N*,*N*-diethyl-3-methylbenzamide (DEET) ([22], but see [23]). Although such a function is difficult to reconcile with the fact that IR40a-expressing neurons are found in sensilla lacking pores [19], this is potentially interesting, as it may suggest a hygrosensory component to the repellent effect of DEET. Yet, we observed no responses to DEET in our *IR40a>GCaMP6m* line (Figure 3N). Thus, it seems unlikely that IR40a (or its orthologs in, e.g., mosquitoes) is the main mediator of DEET avoidance.

Thermosensory and Hygrosensory Responses in the PAL Are Anatomically and Functionally Separable

Localized evaporative cooling has been suggested as a potential mechanism for dry-air responses [5, 24, 25]. Hence, we next tested whether the Arm may also be activated by temperature

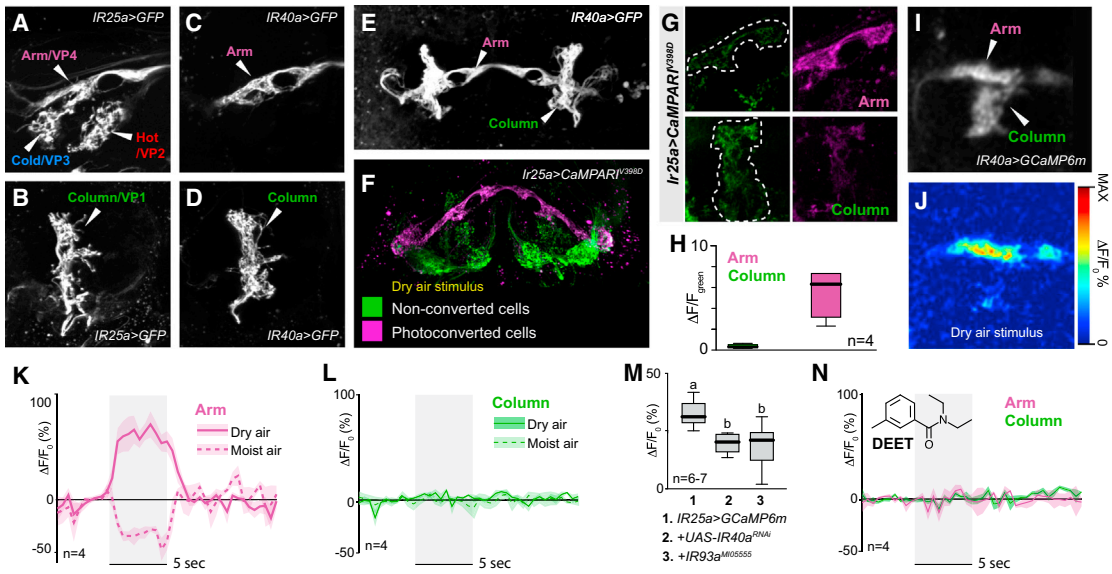

Figure 3. Calcium Responses in the Posterior Antennal Lobe to Humidity Stimuli

(A and B) Maximum-intensity projection from the posterior antennal lobe (PAL) of *IR25a>GFP* brain focusing on Arm (A) and Column (B). Hot and cold glomeruli of the PAL are also visible (A).

(C–E) Maximum-intensity projection from the PAL of *IR40a>GFP* brain focusing on Arm (C) and Column (D) with an overview (E).

(F) Maximum-intensity projection of the antennal lobe from *IR25a>CaMPARI$^{(V398D)}$* flies following photoconversion during dry-air stimulation. See also Figure S3A.

(G) Close-up of Arm and Column showing non-photoconverted (green) and photoconverted (magenta) *IR25a>CaMPARI$^{(V398D)}$* structures in response to dry stimulus.

(H) Boxplot showing quantification of photoconversion ($\Delta F/F_{green}$) in response to dry stimulus in Arm and Column glomeruli of *IR25a>CaMPARI$^{(V398D)}$* flies. The edges of the boxes are the first and third quartiles, thick lines mark the medians, and whiskers represent data range.

(I) Single-optical-plane micrograph from the antennal lobe of an *IR40a>GCaMP6m* fly.

(J) Pseudocolored single-optical-plane micrograph from *IR40a>GCaMP6m* flies responding to dry-air stimulus.

(K and L) Averaged traces from Arm (K) and Column (L) of *IR40a>GCaMP6m* flies stimulated with dry or humid air. Shaded areas represent SEM. Gray bars represent stimulus duration (5 s). See also Figures S3B–S3D.

(M) Boxplot of median peak value to a dry stimulus in Arm of *IR25a>GCaMP6m*, *IR25a>GCaMP6m+IR40a^{RNAi}*, and *IR25a>GCaMP6m+IR93a^{MI05555}*. Differences between mutant and control were tested with one-way ANOVA with Bonferroni correction. b denotes $p < 0.01$, $p = 0.0027$.

(N) Averaged traces from Arm and Column of *IR40a>GCaMP6m* flies stimulated with 10% DEET. Shaded areas represent SEM. The gray bar represents stimulus duration (5 s).

changes. We again turned to calcium imaging and recorded responses of the Arm and Column of *IR25a>GCaMP6m* flies to thermal stimulation (Figures 4A–4C). The Arm glomerulus showed little response to temperature changes (Figure 4B). Slight, cooling-induced [Ca^{2+}] transients could only be observed for cooling steps larger than ~5°C (Figure 4B). This is quite different from the sensitive responses of the hot and cold glomeruli to temperature changes (Figures 4D and 4E; see also [18]). The Column was, however, activated by cooling stimuli of small magnitude (Figure 4C), albeit these responses were still somewhat smaller than those of the cold glomerulus (compare to Figure 4D). Interestingly, whereas targeted *IR40a^{RNAi}* reduced the Arm responses to dry air, the same intervention did not reduce the responses of the Arm and Column to cooling (Figure S4). This suggests that cooling responses in the Arm and Column do not require IR40a, and are therefore unlikely to mediate humidity preference in our assay.

We next wondered whether the cold-induced activity of the Arm or Column contributes to temperature-preference behavior. We silenced IR40a-expressing Arm and Column neurons by expression of the Kir2.1 potassium channel (i.e., by hyperpolarization) under the control of the *IR40a-Gal4* driver, and tested the resulting flies for temperature preference. *IR40a>Kir2.1* flies displayed normal thermal preference (Figure 4F), despite the expected strong defects in humidity preference (Figure 4G). This result indicates that although the Arm and Column respond to cooling stimuli, this activity is not essential for rapid temperature preference. As a control, expression of Kir2.1 under *IR25a-Gal4* (expressed in both the arista and sacculus) resulted in strong defects in both humidity and temperature preference (data not shown and Figure 4F). Together, our data suggest that thermosensory and hygrosensory responses can be genetically and functionally separated in the fly antenna, and that the preference for a suitable relative humidity range involves specialized sacculus neurons that co-express IR40a, IR93a, and IR25a and directly respond to changes in external humidity.

DISCUSSION

Due to their small size and low heat capacity, insects are at constant risk of desiccation. As a result, they have evolved uniquely sensitive receptor systems to sense and respond to changes in the amount of water vapor in the air. Here we describe genes and neurons necessary for hygrosensory responses in the vinegar fly

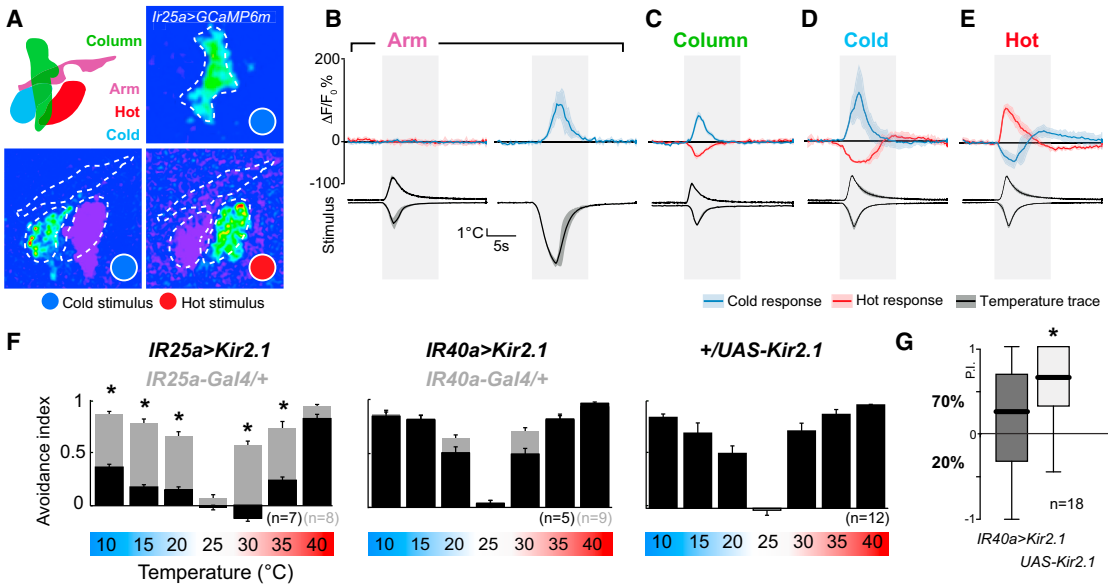

Figure 4. Calcium Responses in the Posterior Antennal Lobe to Temperature Stimuli

(A) Schematic illustration of the PAL and pseudocolored heat maps of response in the PAL to cooling or heating stimuli of *IR25a>GCaMP6m* flies.

(B–E) Averaged traces of calcium responses from PAL glomeruli stimulated with moderate (~3°C) or large (~8°C) temperature stimuli (for each panel, n = 3–5 animals). Baseline temperature for all stimuli is similar (~25°); temperature traces have been systematically offset for illustrative purposes only. Shaded areas represent SD.

(B) Averaged traces of responses from Arm of *IR25a>GCaMP6m* flies stimulated with (left) moderate hot and cold and (right) large cold stimuli. See also Figure S4.

(C) Averaged traces of responses from Column of *IR25a>GCaMP6m* flies stimulated with moderate hot and cold temperature stimuli. See also Figure S4.

(D) Averaged traces of responses from cold (VP3) glomerulus of *IR25a>GCaMP6m* flies stimulated with moderate temperature stimuli.

(E) Averaged traces of responses from hot (VP2) glomerulus of *IR25a>GCaMP6m* flies stimulated with moderate temperature stimuli.

(F) Temperature-avoidance index of *IR25a>Kir2.1*, *IR40a>Kir2.1*, and *UAS-Kir2.1*.

(G) Humidity-preference index of *IR40a>Kir2.1* and *UAS-Kir2.1*.

Temperature-avoidance index values were compared by two-way ANOVA; the asterisks in (F) denote a significant interaction between the Gal4 and UAS transgenes, $p < 0.01$; error bars indicate mean ± SEM. Humidity preference was tested with one-sample t test, theoretical mean 0; asterisks in (G) denote a P.I. significantly different from 0, $p < 0.05$. The edges of the boxes are the first and third quartiles, thick lines mark the medians, and whiskers represent data range.

D. melanogaster. Our work identifies sacculus neurons innervating chambers I and II as essential players in the behavioral responses to environmental humidity. These neurons appear to co-express IR25a, IR93a, and IR40a but, whereas IR25a and IR93a are also required for thermal preference, IR40a is uniquely important for hygrosensory responses. Genetic labeling of *IR40a*-expressing neurons also allowed us to track their projections to the brain and to identify a unique glomerular structure (the Arm) that responds to specific changes in external humidity, i.e., "dry-air" stimuli.

Work in other insects suggests that the neural response to dry air could be mediated by evaporative cooling (as in man-made evaporation detectors, or psychrometers) [5, 24, 25]. Yet, the poor thermal sensitivity of IR40a neurons targeting the Arm (and their unchanged responses to cooling in $IR40a^{RNAi}$) seems to disfavor this model. Furthermore, sensilla responding to changes in humidity have been electrophysiologically characterized in a number of insects [24, 26, 27], and typically consist of a "dry cell" and a "moist cell" (i.e., activated by humid air) housed in the same sensillum together with a "cold cell." We identify here a dry-cell type associated with a cold-responding one in the sacculus. This indicates that hygrosensilla may share a common organization across insect groups.

The results we present here reveal some of the cellular substrates and molecular transducers that allow flies to detect changes in humidity. Interestingly, some of the key molecules we describe seem to be shared between thermosensory and hygrosensory neurons, and yet thermal preference and humidity preference are mediated by independent cellular substrates. Hence, the two sensory systems can function largely in parallel in *Drosophila*, perhaps providing a mechanism to independently modulate the behavioral responses to each of these two key environmental parameters.

SUPPLEMENTAL INFORMATION

Supplemental Information includes four figures and Supplemental Experimental Procedures and can be found with this article online at http://dx.doi.org/10.1016/j.cub.2016.03.049.

AUTHOR CONTRIBUTIONS

A.E., G.S.B.S., M.G., and M.C.S. conceived and designed the study. A.E. performed all humidity experiments and, with assistance from S.M., anatomical studies by confocal microscopy. A.E. performed two-photon Ca^{2+} imaging of humidity responses. E.E.Z. carried out all temperature-preference and two-photon anatomy experiments. D.D.F. performed two-photon Ca^{2+} imaging for temperature responses. A.E., M.G., and M.C.S. analyzed the data and wrote the manuscript with input from all authors.

ACKNOWLEDGMENTS

We wish to thank Dr. Ola Gustafsson for assistance with electron microscopy, Andrew Kuang for technical assistance, and Dr. Thomas Bozza for valuable comments. This work was funded by the Crafoord Foundation (M.C.S.), Vetenskapsrådet (M.C.S.), Birgit och Sven Håkan Ohlssons Stiftelse (M.C.S.), Astrid och Gustaf Kaleens Fond (A.E.), Kungliga Fysiografiska Sällskapet (A.E.), Wenner-Gren Stiftelse (A.E.), NIH R01 grants (NIGMS R01GM08946, NIDCD R01DC01279, and NIDDK R01DK106636), and the Irma T. Hirschl/Weill Caulier Trust Award (to G.S.B.S.). Work in the M.G. laboratory was supported by NIH grant R01NS086859 (to M.G.), the Chicago Biomedical Consortium with support from the Searle Funds at the Chicago Community Trust (to E.E.Z.), and NIH grant F31NS093873 (to D.D.F.).

Received: February 25, 2016
Revised: March 21, 2016
Accepted: March 22, 2016
Published: May 5, 2016

REFERENCES

1. Shelford, V.E. (1918). A comparison of the responses of animals in gradients of environmental factors with particular reference to the method of reaction of representatives of the various groups from protozoa to mammals. Science *48*, 225–230.
2. Okal, M.N., Francis, B., Herrera-Varela, M., Fillinger, U., and Lindsay, S.W. (2013). Water vapour is a pre-oviposition attractant for the malaria vector *Anopheles gambiae* sensu stricto. Malar. J. *12*, 365.
3. von Arx, M., Goyret, J., Davidowitz, G., and Raguso, R.A. (2012). Floral humidity as a reliable sensory cue for profitability assessment by nectar-foraging hawkmoths. Proc. Natl. Acad. Sci. USA *109*, 9471–9476.
4. Sayeed, O., and Benzer, S. (1996). Behavioral genetics of thermosensation and hygrosensation in *Drosophila*. Proc. Natl. Acad. Sci. USA *93*, 6079–6084.
5. Altner, H., and Loftus, R. (1985). Ultrastructure and function of insect thermo- and hygroreceptors. Annu. Rev. Entomol. *30*, 273–295.
6. Winston, P.W., and Bates, D.H. (1960). Saturated solutions for the control of humidity in biological research. Ecology *41*, 232–237.
7. Perttunen, V., and Erkkila, H. (1952). Humidity reaction in *Drosophila melanogaster*. Nature *169*, 78.
8. Liu, L., Li, Y., Wang, R., Yin, C., Dong, Q., Hing, H., Kim, C., and Welsh, M.J. (2007). *Drosophila* hygrosensation requires the TRP channels water witch and nanchung. Nature *450*, 294–298.
9. Ji, F., and Zhu, Y. (2015). A novel assay reveals hygrotactic behavior in *Drosophila*. PLoS ONE *10*, e0119162.
10. Clyne, P.J., Warr, C.G., Freeman, M.R., Lessing, D., Kim, J., and Carlson, J.R. (1999). A novel family of divergent seven-transmembrane proteins: candidate odorant receptors in *Drosophila*. Neuron *22*, 327–338.
11. Vosshall, L.B., Amrein, H., Morozov, P.S., Rzhetsky, A., and Axel, R. (1999). A spatial map of olfactory receptor expression in the *Drosophila* antenna. Cell *96*, 725–736.
12. Benton, R., Vannice, K.S., Gomez-Diaz, C., and Vosshall, L.B. (2009). Variant ionotropic glutamate receptors as chemosensory receptors in *Drosophila*. Cell *136*, 149–162.
13. Larsson, M.C., Domingos, A.I., Jones, W.D., Chiappe, M.E., Amrein, H., and Vosshall, L.B. (2004). Or83b encodes a broadly expressed odorant receptor essential for *Drosophila* olfaction. Neuron *43*, 703–714.
14. Abuin, L., Bargeton, B., Ulbrich, M.H., Isacoff, E.Y., Kellenberger, S., and Benton, R. (2011). Functional architecture of olfactory ionotropic glutamate receptors. Neuron *69*, 44–60.
15. Silbering, A.F., Rytz, R., Grosjean, Y., Abuin, L., Ramdya, P., Jefferis, G.S., and Benton, R. (2011). Complementary function and integrated wiring of the evolutionarily distinct *Drosophila* olfactory subsystems. J. Neurosci. *31*, 13357–13375.
16. Russell, J., Vidal-Gadea, A.G.G., Makay, A., Lanam, C., and Pierce-Shimomura, J.T. (2014). Humidity sensation requires both mechanosensory and thermosensory pathways in *Caenorhabditis elegans*. Proc. Natl. Acad. Sci. USA *111*, 8269–8274.
17. Frank, D.D., Jouandet, G.C., Kearney, P.J., Macpherson, L.J., and Gallio, M. (2015). Temperature representation in the *Drosophila* brain. Nature *519*, 358–361.
18. Gallio, M., Ofstad, T.A., Macpherson, L.J., Wang, J.W., and Zuker, C.S. (2011). The coding of temperature in the *Drosophila* brain. Cell *144*, 614–624.
19. Shanbhag, S.R., Singh, K., and Singh, R.N. (1995). Fine structure and primary sensory projections of sensilla located in the sacculus of the antenna of *Drosophila melanogaster*. Cell Tissue Res. *282*, 237–249.
20. Stocker, R.F., Lienhard, M.C., Borst, A., and Fischbach, K.F. (1990). Neuronal architecture of the antennal lobe in *Drosophila melanogaster*. Cell Tissue Res. *262*, 9–34.
21. Fosque, B.F., Sun, Y., Dana, H., Yang, C.-T.T., Ohyama, T., Tadross, M.R., Patel, R., Zlatic, M., Kim, D.S., Ahrens, M.B., et al. (2015). Labeling of active neural circuits in vivo with designed calcium integrators. Science *347*, 755–760.
22. Kain, P., Boyle, S.M., Tharadra, S.K., Guda, T., Pham, C., Dahanukar, A., and Ray, A. (2013). Odour receptors and neurons for DEET and new insect repellents. Nature *502*, 507–512.
23. Xu, P., Choo, Y.-M.M., De La Rosa, A., and Leal, W.S. (2014). Mosquito odorant receptor for DEET and methyl jasmonate. Proc. Natl. Acad. Sci. USA *111*, 16592–16597.
24. Tichy, H., and Loftus, R. (1996). Hygroreceptors in insects and a spider: humidity transduction models. Naturwissenschaften *83*, 255–263.
25. Tichy, H., and Kallina, W. (2013). The evaporative function of cockroach hygroreceptors. PLoS ONE *8*, e53998.
26. Merivee, E., Must, A., Luik, A., and Williams, I. (2010). Electrophysiological identification of hygroreceptor neurons from the antennal dome-shaped sensilla in the ground beetle *Pterostichus oblongopunctatus*. J. Insect Physiol. *56*, 1671–1678.
27. Piersanti, S., Rebora, M., Almaas, T.J., Salerno, G., and Gaino, E. (2011). Electrophysiological identification of thermo- and hygro-sensitive receptor neurons on the antennae of the dragonfly *Libellula depressa*. J. Insect Physiol. *57*, 1391–1398.